J. Fluid Mech. (1982), *vol.* 115, *pp.* 303–314
Printed in Great Britain

Bend theory of river meanders. Part 2. Nonlinear deformation of finite-amplitude bends

By GARY PARKER

St Anthony Falls Hydraulic Laboratory, University of Minnesota, Minneapolis, Minnesota, 55414, USA

KENJI SAWAI

Disaster Prevention Research Institute, Kyoto University, Uji, Japan

AND SYUNSUKE IKEDA

Department of Foundation Engineering, Saitama University, Saitama, Japan

(Received 31 December 1979 and in revised form 26 June 1981)

Meander bends typically show certain systematic deviations from simple Cartesian sinusoidal forms. Bends tend to be round and full, or 'fat', often to the point of possessing double-valued plan-forms, as Langbein & Leopold (1966) have noted. Bends also tend to be characteristically skewed in such a fashion that their direction of migration can be determined directly from an aerial photograph of the planform; the water margin of the downstream accreting half of a point bar describes a convex planform, whereas the upstream eroding side has a concave shape.

In the present paper a generalized nonlinear equation of bend migration is treated based on the analysis of Part 1 (Ikeda, Parker & Sawai 1981). An expansion technique reminiscent of the Stokes expansion for water waves is developed to perform a nonlinear stability analysis. This analysis provides an explanation of skewing and fattening, and also indicates that lateral and downstream migration rates should increase as bend amplitude develops. These results agree qualitatively with field observations.

1. Introduction

The linear theory of bend instability presented in Part 1 of this work (Ikeda, Parker & Sawai 1981) provides a description of the initial growth and downstream migration of sinusoidal channel meandering of infinitesimal amplitude. In the case of finite-amplitude bends, however, nonlinear effects may be presumed to cause modification of growth and migration rates, and to deform the bends in some characteristic way. This nonlinear problem is approached herein.

Before embarking on a formal analysis, it is perhaps useful to categorize heuristically two ways in which natural meanders differ from the simple sinusoidal pattern used in the preceding linear analysis, viz.

$$y = \epsilon \cos kx \tag{1}$$

(equation (17) at $t = 0$ therein; only parameters that do not appear in the preceding paper are defined herein). The first systematic deviation may be termed 'fatness'; it is implicit in the 'sine-generated curve' of Langbein & Leopold (1966). They noted

that the bends of many meandering streams are so round and full (i.e. 'fat') that the Cartesian representation $y = y(x)$ is not single-valued (figure 1). They suggested that specifying the curve in intrinsic co-ordinates as

$$\theta = -\theta_{\max} \sin \kappa s, \tag{2}$$

where θ is angle, s is arc length, $\theta_{\max}$ is the angular amplitude, and κ is the arc-length, or intrinsic meander wavenumber (all parameters made dimensionless after the fashion of the preceding paper), provides a much better representation. The rather extreme value of $\theta_{\max}$ of 115° is used in figure 1*a* to illustrate (2).

Equation (2) can be converted to Cartesian co-ordinates via the nonlinear transformations

$$\theta = \tan^{-1}\left(\frac{\partial y}{\partial x}\right), \quad \frac{\partial s}{\partial x} = \left\{1 + \left(\frac{\partial y}{\partial x}\right)^2\right\}^{\frac{1}{2}} \equiv \gamma^{-1}, \tag{3}$$

where $\gamma \equiv \cos\theta$. The case of small-amplitude meandering, in the sense that

$$\delta_0 = k\epsilon \ll 1,$$

provides an illustration of the fattening implicit in equation (2). Transformed to Cartesian co-ordinates, it becomes

$$y = \epsilon[\cos kx - \delta_0^2 J_F \cos 3kx + o(\delta_0^3)], \tag{4a}$$

where $J_F = 7/144$, and

$$\epsilon = \frac{\theta_{\max}}{k}[1 + \tfrac{3}{16}\delta_0^2 + o(\delta_0^3)], \tag{4b}$$

$$k = \kappa[1 + \tfrac{1}{4}\delta_0^2 + o(\delta_0^3)]. \tag{4c}$$

Thus the geometric nonlinear transformation from (2) to (4*a*) involves the generation of higher-order modes. The role of the third-order term containing J_F in (4*a*) is to fatten the base mode, and thus it is called the 'Cartesian coefficient of fattening' herein. Although the specific value of J_F associated with the sine-generated curve is given by 7/144, it is clear that any positive choice provides fattening (figure 1*b*).

Meander bends also differ systematically from simple sinusoidal waves in a second, little-mentioned way. Bends that are actively migrating downstream tend to show a marked asymmetry in shape that allows one to determine the direction of migration (and thus flow) directly from an aerial photograph. This inherent skewing is schematized in figure 2, in which a line has been drawn so as to bisect a point bar into upstream and downstream portions. The bar is seen to possess a convex bank outline on one side and a concave outline on the other side. Typically the convex side is an area of sediment accretion, often marked by scroll bars; the concave side is usually being eroded. If the bend is to migrate downstream, the accreting convex side must be downstream of the eroding concave side. Skewing is apparent in both the free meanders of figure 3*a* and the confined meanders of figure 3*b*.

While skewing has been noted in passing by many, only a few authors have attached any significance to it. Kinoshita (1961) has documented its ubiquitousness, and has qualitatively associated its formation with points of low downstream migration speed, located between bend apexes and turning points. Narai (1975) employed a numerical analysis in an early attempt to explain it.

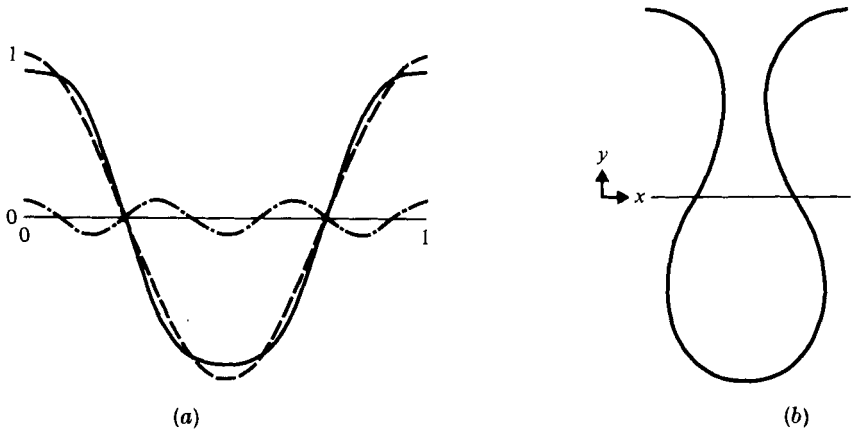

FIGURE 1. (*a*) The sine-generated curve for $\theta_{max} = 115°$. (*b*) Subtraction of the third-mode term ($0{\cdot}1 \cos 3kx$) from the first-mode term ($\cos kx$) yields a rounder, fatter curve.

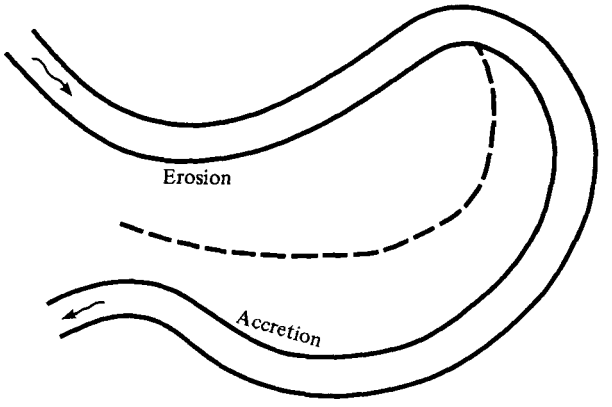

FIGURE 2. A typical bend and point bar illustrating skewing.

Heuristically, skewing in Cartesian co-ordinates of fairly small-amplitude bends can be described by adding another third-mode term to equation (4*a*); to $O(\delta_0^2)$, it becomes

$$y = \epsilon(\cos kx - \delta_0^2 J_F \cos 3k - \delta_0^2 J_S \sin 3kx). \tag{5}$$

Here J_S is the 'Cartesian coefficient of skewing'; it must be positive for flow in the positive x direction. The choices $\delta_0 = 0{\cdot}98$, $J_F = 0{\cdot}073$, $J_S = 0{\cdot}103$ provide a fairly accurate representation of a reach of the Beaver River, Canada of figure 3*b*; this is shown in figure 4.

A mechanism which leads to the production of higher Fourier modes from a base mode without external excitation must be nonlinear. Herein an expansion technique is developed for the nonlinear bend equation of the preceding paper; its application allows for an explanation of fattening and skewing, in addition to indicating the effects of the nonlinear terms on the growth and migration rates of bends.

(*a*)

(*b*)

FIGURE 3. (*a*) A reach of the Pembina River, Alberta, Canada.
(*b*) A reach of the Beaver River, Alberta, Canada.

FIGURE 4. The dashed line represents the observed centre-line of the reach of the Beaver River in figure 3*a*; the solid line represents the approximation provided by equation (5) with $\delta = 0{\cdot}98$, $J_F = 0{\cdot}073$ and $J_S = 0{\cdot}103$.

2. The nonlinear expansion

The expansion technique used herein to perform a nonlinear stability analysis is similar to the Stokes expansion for finite-amplitude water waves (see, for example, Whitham 1974).

Before embarking on the analysis, however, it is useful to have a criterion for determining the initial stability characteristics of an equation that can apply to nonlinear as well as linear equations. Let $y = 0 + y'$, where y' is a perturbation assumed to be periodic in x with wavenumber k. The root-mean-square amplitude of the perturbation is defined to be y^*, where

$$y^{*2} = \frac{k}{2\pi}\int_0^{2\pi/k} y'^2 dx.$$

A bulk growth rate α_B can then be defined at $t = 0$;

$$\frac{1}{y^*}\frac{dy^*}{dt}\bigg|_{t=0} = \alpha_B. \tag{6}$$

The parameter α_B provides an unambiguous indication as to whether or not a perturbation tends to grow or die in amplitude at $t = 0$, regardless of whether or not y' refers to an infinitesimal or finite-amplitude perturbation.

The nonlinear bend equation (15) in the analysis of Part 1, takes the form

$$\frac{\partial}{\partial x}\left(\gamma\frac{\partial y}{\partial t}\right) + 2\chi C_f\frac{\partial y}{\partial t} = \{1+e(\chi-1)\}\left\{\chi\frac{\partial}{\partial x}\left(\gamma^3\frac{\partial^2 y}{\partial x^2}\right) - C_f(F^2\chi^5 + \tilde{A}\chi^2)\,\gamma^2\frac{\partial^2 y}{\partial x^2}\right\}, \tag{7}$$

where $\tilde{A} = A + F^2$, A is equal to 2·89 for alluvial meanders, F is Froude number and C_f is a friction coefficient of the unperturbed flow, e is a constant expected to be positive, and

$$\gamma = \cos\theta = \frac{1}{\left\{1+\left(\dfrac{\partial y}{\partial x}\right)^2\right\}^{\frac{1}{2}}}, \quad \chi = \overline{(\gamma^{-1})}^{-\frac{1}{3}}.$$

These terms provide nonlinear coupling between reach-averaged and fluctuating flows; they account for the increase in channel sinuosity and consequent decrease in slope as bend amplitude increases.

The derivation of the nonlinear bend equation involved the neglect of $O(\nu^3)$ dynamic nonlinearities. The following analysis accounts for $O(\delta_0^3)$ geometric nonlinearities. The neglect of the former but the retention of the latter is justified if $(\nu/\delta_0)^3 \ll 1$. For bends of small amplitude

$$\nu = \frac{b}{r_0} \simeq \frac{(2\pi)^2 b y_0}{\lambda^2}, \quad \delta_0 = \frac{2\pi y_0}{\lambda},$$

so that

$$\left(\frac{\nu}{\delta_0}\right)^3 \simeq \left(\frac{2\pi b}{\lambda}\right)^3.$$

A typical ratio of meander bend wavelength to half-width is about 20, so that the approximation is justified.

The linear stability of (6) can be examined with the perturbation

$$y = \epsilon\mu_1(x,t), \tag{8a}$$

where

$$\mu_1 = e^{\alpha_0 t}\cos(kx - \omega_0 t) \tag{8b}$$

and $\epsilon \ll 1$. Clearly $\alpha_0 = \alpha_B$, as would be expected.

The method of Stokes for finite-amplitude water waves suggests the following expansion for the nonlinear case;

$$y = \epsilon\mu_1(\tau,\phi) + \epsilon^3\mu_3(\tau,\phi) + \dots, \tag{9}$$

where

$$\tau = \alpha t, \quad \phi = kx - \omega t, \tag{10}$$

and

$$\alpha = \alpha_0 + \epsilon^2\alpha_2 + \dots, \quad \omega = \omega_0 + \epsilon^2\omega_2 + \dots. \tag{11}$$

In fact, it is possible to obtain a valid expansion for small time by the use of an unstrained expansion, i.e. one with α_2 and ω_2 equal to zero. The straining implicit in (11), however, provides an explicit description of the variation of rates of migration and growth with amplitude.

The above expansion procedure is now applied to (7). Noting that

$$\gamma = 1 - \tfrac{1}{2}k^2\epsilon^2\mu_1'^2 + \dots,$$
$$\chi = 1 - \tfrac{1}{6}k^2\epsilon^2\overline{\mu_1'^2} + \dots,$$

the $O(\epsilon)$ and $O(\epsilon^3)$ expansions of the nonlinear bend equation are found to be

$$\mathscr{L}(\mu_1) = 0, \tag{12}$$

$$\mathscr{L}(\mu_3) = \tfrac{1}{2}k^3\{\mu_1'^2(\alpha_0\dot{\mu}_1 - \omega_0\mu_1')\}' - \tfrac{3}{2}k^5(\mu_1'^2\mu_1'')' + C_f\tilde{A}k^4\mu_1'^2\mu_1'' - \left(k\frac{\partial}{\partial\phi} + 2C_f\right)(\alpha_2\dot{\mu}_1 - \omega_2\mu_1')$$
$$+ \overline{\mu_1'^2}\{\tfrac{1}{3}C_fk^2(\alpha_0\dot{\mu}_1 - \omega_0\mu_1') - \tfrac{1}{6}k^5(1+e)\mu_1''' + \tfrac{1}{6}C_fk^4W\mu_1''\}. \tag{13}$$

In the above, $\cdot = \partial/\partial\tau$ and $' = \partial/\partial\phi$, and the linear operator $\mathscr{L}$ is given by

$$\mathscr{L} = \left(k\frac{\partial}{\partial\phi} + 2C_f\right)\left(\alpha_0\frac{\partial}{\partial\tau} - \omega_0\frac{\partial}{\partial\phi}\right) - \left(k\frac{\partial}{\partial\phi} - C_f\tilde{A}\right)k^2\frac{\partial^2}{\partial\phi^2} \tag{14}$$

and

$$W = F^2(5+e) + A(2+e).$$

Equation (12) yields the linear solution of Part 1, viz.

$$\mu_1 = e^\tau\cos\phi, \tag{15}$$

$$\alpha_0 = -\frac{(k^4 - 2C_f^2\tilde{A}k^2)}{k^2 + 4C_f^2}, \quad \omega_0 = \frac{2C_fk^3(1+\frac{1}{2}\tilde{A})}{k^2+4C_f^2}. \tag{16}$$

Initial growth-rate α_0 is maximized at the characteristic meander wavenumber $k = k_{0M}$, where

$$k_{0M} = \beta C_f \tag{17}$$

and $\beta = 2\{-1 + (1+\frac{1}{2}\tilde{A})^{\frac{1}{2}}\}^{\frac{1}{2}}$. At this value of k, α_0 and ω_0 take the values

$$\alpha_{0M} = \tfrac{1}{4}k_{0M}^2\beta^2, \quad \omega_{0M} = \tfrac{1}{2}k_{0M}^2\beta\left(1 + \frac{\beta^2}{4}\right) \tag{18}$$

and

$$c_{0M} = \omega_{0M}/k_{0M}.$$

For the case of alluvial meanders satisfying the conditions $F^2 \ll 1$, β is found to approximate to 1·50. Information presented in Part 1 suggests that $A \cong 0$ in the incised case; thus for $F^2 \ll 1$ it is found that $\beta \cong F$.

Equations (15) and (16) may be used to reduce (13) to the form

$$\mathscr{L}(\mu_3) = \{e^{3\tau}(\tfrac{3}{8}k^3\omega_0 - \tfrac{1}{12}W_2C_fk^4 + \tfrac{1}{6}C_fk^2\alpha_0) - e^\tau(k\omega_2 + 2C_f\alpha_2)\}\cos\phi$$
$$+ \{e^{3\tau}(-\tfrac{1}{8}k^3\alpha_0 - \tfrac{1}{24}W_3k^5 + \tfrac{1}{6}C_fk^2\omega_0) - e^\tau(-k\alpha_2 + 2C_f\omega_2)\}\sin\phi$$
$$+ e^{3\tau}\{(-\tfrac{3}{8}k^3\omega_0 + \tfrac{1}{4}C_f\tilde{A}k^4)\cos 3\phi + (\tfrac{3}{8}k^3\alpha_0 + \tfrac{9}{8}k^5)\sin 3\phi\}, \tag{19}$$

where $W_2 = F^2(8+e) + A(5+e)$ and $W_3 = 11 + 2e$. Note that third-mode terms have been generated in the right-hand side of the above equation; these are the results of nonlinear interaction associated with skewing and fattening.

The reason for pursuing a Stokes-type analysis is the possibility of quantifying conveniently the effect of nonlinearities on the growth-rate and migration rate via α_2 and ω_2. According to the Stokes technique, α_2 and ω_2 are chosen so as to make the first-mode terms vanish from the right-hand side of (19). However, it is apparent from the equation that no constant value of α_2 and ω_2 can be found so as to accomplish this due to the difference between the exponential terms e^{τ} and $e^{3\tau}$. Thus the use of a Stokes-type straining fails. Rather than resort to an unstrained expansion to solve the problem, the straining technique is modified in the next section.

3. Modified expansion

Herein the Stokes technique is modified as follows. It is assumed that, instead of (11),

$$\alpha(\tau) = \alpha_0 + \epsilon^2\alpha_2\mathscr{F}(\tau) + \ldots, \quad \omega(\tau) = \omega_0 + \epsilon^2\omega_2\mathscr{F}(\tau) + \ldots, \tag{20}$$

where $\mathscr{F}(0) = 1$ and $\mathscr{F}(\tau)$ is chosen such that up to $O(\epsilon^2)$

$$\frac{\partial}{\partial t} = (\alpha_0 + \epsilon^2\alpha_2 e^{2\tau})\frac{\partial}{\partial \tau} - (\omega_0 + \epsilon^2\omega_2 e^{2\tau})\frac{\partial}{\partial \phi}. \tag{21}$$

After some manipulation the correct choice is found to be

$$\mathscr{F}(\tau) = \frac{e^{2\tau} - 1}{2\tau}. \tag{22}$$

An expansion of (7) with the aid of (9), (10) and (20) then yields (12) and

$$\mathscr{L}(\mu_3) = \tfrac{1}{2}k^3\{\mu_1'^2(\alpha_0\dot{\mu}_1 - \omega_0\mu_1')\}' - \tfrac{3}{2}k^5(\mu_1'^2\mu_1'')' + C_f\tilde{A}k^4\mu_1'^2\mu_1'' - e^{2\tau}\left(k\frac{\partial}{\partial\phi} + 2C_f\right)$$
$$(\alpha_2\dot{\mu}_1 - \omega_2\mu_1') + \overline{\mu_1'^2}\{\tfrac{1}{3}C_f k^2(\alpha_0\dot{\mu}_1 - \omega_0\mu_1') - \tfrac{1}{6}k^5(1+e)\mu_1''' + \tfrac{1}{6}C_f k^4 W\mu_1''\}. \tag{23}$$

This equation can be rewritten with the aid of (15), (16a) and (16b) as

$$\mathscr{L}(\mu_3) = e^{3\tau}[\{\tfrac{3}{8}k^3\omega_0 - \tfrac{1}{12}W_2C_f k^4 + \tfrac{1}{6}C_f k^2\alpha_0 - (k\omega_2 + 2C_f\alpha_2)\}\cos\phi +$$
$$\{-\tfrac{1}{8}k^3\alpha_0 - \tfrac{1}{24}W_3k^5 + \tfrac{1}{6}C_f k^2\omega_0 - (-k\alpha_2 + 2C_f\omega_2)\}\sin\phi$$
$$+ (-\tfrac{3}{8}k^3\omega_0 + \tfrac{1}{4}C_f\tilde{A}k^4)\cos 3\phi + (\tfrac{3}{8}k^3\alpha_0 + \tfrac{9}{8}k^5)\sin 3\phi]. \tag{24}$$

In the above equation the temporal functionality takes the form $e^{3\tau}$, and thus it is possible to find values of α_2 and ω_2 so as to cause the first-mode terms to vanish from the right-hand side.

4. Nonlinear effects on growth-rate and downstream migration rate

In order to eliminate first-mode terms from the right-hand side of (24), α_2 and ω_2 must take the forms

$$\alpha_2 = \frac{\frac{1}{24}W_3k^6 + k^4(\frac{1}{8}\alpha_0 - \frac{1}{6}C_f^2W_2) + \frac{7}{12}C_f k^3\omega_0 + \frac{1}{3}C_f^2k^2\alpha_0}{k^2 + 4C_f^2}, \tag{25a}$$

$$\omega_2 = \frac{-\frac{1}{12}(W_2 + W_3)C_f k^5 + \frac{3}{8}k^4\omega_0 - \frac{1}{12}C_f k^3\alpha_0 + \frac{1}{3}C_f^2k^2\omega_0}{k^2 + 4C_f^2}. \tag{25b}$$

The effects of nonlinear interaction on the behaviour of perturbations at the wavenumber k_{0M}, associated with maximum initial instability according to the linear theory, can now be quantified. It is seen from (20) and (22) that

$$\alpha(0) = \alpha_0 + \epsilon^2\alpha_2 + \ldots, \quad \omega(0) = \omega_0 + \epsilon^2\omega_2 + \ldots .$$

The above two relations and equations (16a), (16b), (17), (18a), and (18b) yield the forms for $\alpha(0)$ and $\omega(0)$ at $k = k_{0M}$

$$\alpha(0)|_{k_{0M}} = \alpha_{0M}\left(1 - \tfrac{1}{24}\delta_{0M}^2 \frac{2e + 12f + \frac{1}{2}e\beta^2}{1 + \frac{1}{4}\beta^2}\right), \tag{26a}$$

$$\omega(0)|_{k_{0M}} = \omega_{0M}\left\{1 - \tfrac{1}{24}\delta_{0M}^2 \frac{(9 + 2e) + \frac{1}{2}(5 + 2e + 6f)\beta^2 + \frac{1}{16}(1 + 2e)\beta^4}{(1 + \frac{1}{4}\beta^2)^2}\right\}. \tag{26b}$$

Likewise $c(0)|_{k_{0M}} = \omega(0)|_{k_{0M}}/k_{0M}$. In the above relations $\delta_{0M} = k_{0M}\epsilon$ and f is defined by

$$f = F^2/\beta^2. \tag{27}$$

It is seen from (26a) and (26b) that nonlinear effects reduce both the coefficient of instability and migration rate of bends at the meander length associated with maximum linear instability. The true nature of the expansion as one in $\delta_{0M} = k_{0M}\epsilon$ rather than ϵ itself becomes apparent in these two relations.

However, the value of $\alpha(0)$ itself in (26a) is modified by the nonlinear contribution α_2, and so the value of k at which $\alpha(0)$ is maximized should be altered accordingly by $o(\delta_{0M}^2)$. With this in mind, let k_M equal the value of k at which $\alpha(0)$ is a maximum. One would expect that as a result of nonlinear effects

$$k_M = k_{0M} + \epsilon^2 k_{2M} + \ldots . \tag{28}$$

By definition

$$\left.\frac{\partial\alpha(0)}{\partial k}\right|_{k_M} = 0.$$

But from the linear theory $\partial\alpha_0/\partial k|_{k_{0M}} = 0$; thus to second order

$$\left.\frac{\partial\alpha(0)}{\partial k}\right|_{k_{0M}+\epsilon^2 k_{2M}} = \epsilon^2\left(\left.\frac{\partial^2\alpha_0}{\partial k^2}\right|_{k_{0M}} k_{2M} + \left.\frac{\partial\alpha_2}{\partial k}\right|_{k_{0M}}\right) = 0,$$

or

$$k_{2M} = -\left(\frac{\partial\alpha_2}{\partial k}\Big/\frac{\partial^2\alpha_0}{\partial k^2}\right)\Big|_{k_{0M}}. \tag{29}$$

From (16a), (25a), (28) and (29) it is found that

$$k_M = k_{0M}\left\{1 + \tfrac{1}{192}\delta_{0M}^2 \frac{(32 - 4e - 48f) + (8 - 2e - 6f)\beta^2 - \frac{1}{4}e\beta^4}{(1 + \frac{1}{4}\beta^2)}\right\}. \tag{30}$$

The instability coefficient associated with this new characteristic wavenumber at $\tau = 0$ is found to be identical to second order with (26a). Frequency $\omega(0)|_{k_M}$ and meander migration speed $c(0)|_{k_M}$ are modified, however; after some calculation it is found that

$$\omega(0)|_{k_M} = \omega_{0M}[1 + \tfrac{1}{192}\{(24 - 28e - 144f) + (12 - 15e - 54f)\beta^2 + (\tfrac{3}{2} - \tfrac{9}{4}e - \tfrac{3}{2}f)\beta^4 - \tfrac{1}{16}e\beta^6\}/(1 + \tfrac{1}{4}\beta^2)^2], \tag{31}$$

$$c(0)|_{k_M} = c_{0M}\left\{1 - \tfrac{1}{192}\delta_{0M}^2 \frac{(8 + 24e + 96f) + (4 + 12e + 36f)\beta^2 + (\frac{1}{2} + \frac{3}{2}e)\beta^4}{(1 + \frac{1}{4}\beta^2)^2}\right\}. \tag{32}$$

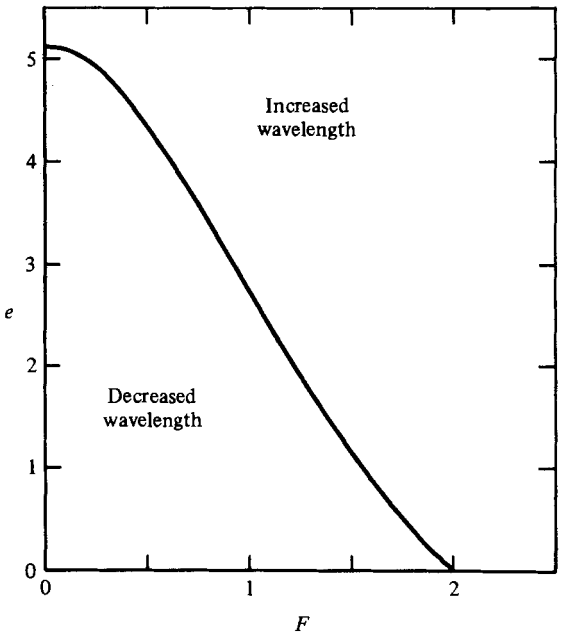

FIGURE 5. Plot of F versus e denoting regions where nonlinear effects act to increase or decrease alluvial meander wavelength.

A complete picture of the effect of geometric nonlinearities on channel migration rates up to $O(\delta_{0M}^2)$ can be obtained from (26a), (30) and (32). Since $f = F^2/\beta^2$ is, and e is assumed to be, non-negative, the first of these indicates that the growth-rate, i.e. the lateral migration rate, should be less in the finite-amplitude case than in the linear theory. Likewise, from (32), the downstream migration rate should be reduced below the linear value.

The characteristic meander wavenumber k_M shows somewhat more complicated behaviour; depending on the value of e and f, k_M may be greater than or less than the linear value. Two cases are of special interest. In Part 1 evidence was quoted to the effect that $A = 0$ and thus $\tilde{A} = F^2$ in the expression for β, for the treatment of incised meanders. It is found from (30) that k_M is always less than k_{0M} for this case. On the other hand, the approximate value $A = 2{\cdot}89$ can be used to describe alluvial meanders. In this case $k_M < k_{0M}$ (and meander wavelength exceeds that of the linear theory) only if e is sufficiently large; for $F \ll 1$, e must exceed 5·1, and for $F = 1$, e must exceed 2·7 (figure 5). Otherwise, k_M exceeds k_{0M}, and the meander wavelength of the non-linear theory is less than that of the linear theory.

It should be noted that the expansion technique used herein describes the effect of amplitude on initial rates of lateral and down-stream migration. It does not extend to validity of the expansion in time.

5. Fattening and skewing

The parameters α_2 and ω_2 were chosen so as to cause the first-mode inhomogeneous terms in (24) to vanish; thus the third-mode terms remain. The particular solution to (24) is found to be

$$\mu_3 = -(J_F \cos 3\phi + J_S \sin 3\phi)\, k^2 e^{3\tau}, \tag{33}$$

where

$$J_F = \begin{vmatrix} B_1 & D_2 \\ B_2 & D_1 \end{vmatrix} \Big/ \begin{vmatrix} D_1 & D_2 \\ -D_2 & D_1 \end{vmatrix}, \quad J_S = \begin{vmatrix} D_1 & B_1 \\ -D_2 & B_2 \end{vmatrix} \Big/ \begin{vmatrix} D_1 & D_2 \\ -D_2 & D_1 \end{vmatrix}$$

and

$$B_1 = \tfrac{1}{16} k_{0M}^3 \beta \{4(1+\tfrac{1}{8}\beta^2)\, l^2 - 3(1+\tfrac{1}{4}\beta^2)\, \tilde{\omega}_0 l\}$$

$$B_2 = \tfrac{1}{32} k_{0M}^3 \{36 l^3 + 3\beta^2 \tilde{\alpha}_0 l\}$$

$$D_1 = \tfrac{3}{2} k_{0M}^3 \beta \{6(1+\tfrac{1}{8}\beta^2)\, l^2 - 3(1+\tfrac{1}{4}\beta^2)\, \tilde{\omega}_0 l - \tilde{\alpha}_0\}$$

$$D_2 = -\tfrac{3}{2} k_{0M}^3 \{18 l^3 + \tfrac{3}{2}\beta^2 \tilde{\alpha}_0 l - 2(1+\tfrac{1}{4}\beta^2)\, \tilde{\omega}_0\}.$$

In the above,

$$l = k/k_{0M}, \quad \tilde{\alpha}_0 = \alpha_0/\alpha_{0M}, \quad \tilde{\omega}_0 = \omega_0/\omega_{0M}.$$

J_F and J_S may be evaluated at the characteristic wavenumber by setting $k = k_M$, in which case $l = \tilde{\alpha}_0 = \tilde{\omega}_0 = 1 + O(\delta_{0M}^2)$; it is found that, if $J_{FM} = J_F|_{k_M}$ and $J_{SM} = J_S|_{k_M}$,

$$J_{FM} = \frac{1}{48}\left(\frac{576 + 88\beta^2 + 2\beta^4}{256 + 36\beta^2 + \beta^4}\right) + O(\delta_{0M}^2), \tag{34a}$$

$$J_{SM} = \frac{1}{48}\beta\left(\frac{40 + 12\beta^2 + \tfrac{1}{2}\beta^4}{256 + 36\beta^2 + \beta^4}\right) + O(\delta_{0M}^2). \tag{34b}$$

Replacing these forms into (9), (10), (20), (15), (16a), (16b) and (17), it is found that the complete solution evaluated at the characteristic wavenumber k_M takes the form

$$y = \epsilon[e^{\alpha_M t}\cos(k_M x - \omega_M t) - \delta_{0M}^2 e^{3\alpha_M t}\{J_{FM}\cos 3(k_M x - \omega_M t) + J_{SM}\sin 3(k_M x - \omega_M t)\}] \tag{35}$$

up to $O(\delta_{0M}^2)$. In the above k_M, α_M and ω_M can be obtained from (30), (26a) and (31), respectively, by replacing δ_{0M}^2 therein with $\delta_{0M}^2 \mathscr{F}(\tau)$.

A comparison of equations (5) and (35) reveals that J_{FM} and J_{SM} are indeed the coefficients of fattening and skewing, respectively, at $t = 0$. Equations (34a) and (34b) indicate that both coefficients are positive, in accordance with the observations of the introduction.

Justification of the identification of k_M with the characteristic meander wavenumber requires a proof of the identity of $\alpha(\tau)$ for small time (i.e. $\tau \cong 0$) and the bulk growth-rate α_B given in (6); this is easily established up to order δ_{0M}^2.

6. Summary and qualitative interpretation

The analysis predicts the following nonlinear effects on bend development.

(1) Reduction in lateral and downstream migration rates below the values predicted by the linear theory. The reduction is intensified as time passes and $\mathscr{F}(\tau)$ increases.

(2) The development of positive fattening and skewing; this development is in-

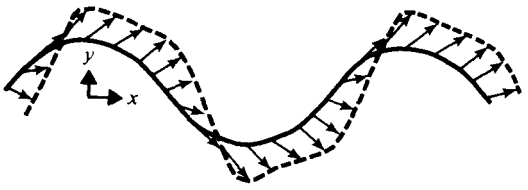

FIGURE 6. Plots of the relation

$$y = e^t \cos \tfrac{1}{3}\pi(x - \tfrac{1}{9}t) - e^{3t}\{0{\cdot}05 \cos \pi(x - \tfrac{1}{9}t) + 0{\cdot}05 \sin \pi(x - \tfrac{1}{9}t)\} \quad \text{at} \quad t = 0$$

(the solid line) and at $t = 0{\cdot}45$ (the dashed line) provide a qualitative illustration of the channel deformation predicted by equation (35).

tensified as time passes. This process is schematized in figure 6, in which a meandering reach intensifies its fattening and skewing as lateral and downstream migration progress.

(3) An increase in characteristic meander wavelength for the case of incised meanders: either an increase or a decrease for the case of alluvial meanders, the former applying for sufficiently large e or F and the latter for sufficiently small e or F.

The first conclusion is supported by the general observation that meander migration eventually slows as amplitude increases; Kinoshita (1961) has observed this in alluvial streams.

The second conclusion agrees with the qualitative description of actual alluvial bends presented in the introduction, and is the most significant result of the analysis.

The third conclusion is the only one that is dependent on the numerical values of e and F. A test of its validity is made difficult for two reasons. First, the exact value of e is as yet unspecified, although it is expected to be positive. Secondly, no systematic change in wavelength as bends increase their amplitude seems to have been clearly documented for either the incised or alluvial case. Thus this point remains unresolved at present.

Figure 6 shows two more features of interest. As bends develop according to equation (35), a point of least apparent migration is seen to appear just upstream of each bend apex. Furthermore the turning point upstream of the apex is seen to migrate toward this point of least apparent migration. Kinoshita (1961) vividly described this process in natural streams.

A final point is of coincidental interest. For the case $F^2 \ll 1$, (34a) yields a value of initial coefficient of fatness $J_F \cong 0{\cdot}0478$ for alluvial meanders and 0·0469 for incised meanders. The corresponding value from the sine-generated curve for the case $\delta_0^2 \ll 1$ is seen from equation (4a) to be equal to 0·0486.

The above co-operative research effort is an outgrowth of a visit by the senior author to several Japanese research establishments. K. Ashida and M. Michiue made the visit possible and are deeply thanked. Much of the actual research was performed at the California Institute of Technology with the kind aid and encouragement of N. Brooks. R. Kinoshita provided the authors with extensive descriptions of natural streams. Y. Seki of Saitama University provided the authors with encouragement and much useful literature. D. Drew, D. Joseph, G. Whitham and A. Chwang made helpful comments concerning the expansion technique. Funding was generously provided by the National Sciences and Engineering Research Council of Canada, and grant number ENG 77-10182 of the U.S. National Science Foundation.

REFERENCES

IKEDA, S., PARKER, G. & SAWAI, K. 1981 Bend theory of river meanders. Part I. Linear development. *J. Fluid Mech.* **112**, 363–377.

KINOSHITA, R. 1961 An investigation of channel deformation of the Ishikari River. Publication no. 36, Natural Resources Division, Ministry of Science and Technology of Japan, 139 pp. (in Japanese).

LANGBEIN, W. B. & LEOPOLD, L. B. 1966 River meanders – theory of minimum variance. U.S. Geological Survey Professional Paper 422H.

NARAI, S. 1975 On the trajectory of fluvial meanders. Proceedings of 30th Annual Meeting of the Japan Society of Civil Engineers, pp. 362–363 (in Japanese).

WHITHAM, G. B. 1974 *Linear and Nonlinear Waves.* John Wiley.